Military Technical College
Kobry El-Kobbah,
Cairo, Egypt.

13th International Conference on Applied Mechanics and Mechanical Engineering.

THREE- LAYERED ELASTIC COMPOSITE WITH SURFACE CRACKS SUBJECTED TO CONVECTIVE COOLING

RIZK* A.A.

ABSTRACT

The Thermoelastic problem for homogenous layer bonded to two similar coated layers with two surface cracks located symmetrically in the outer layers under transient thermal stresses is considered. The transient thermal stresses are generated due to quenching the surfaces containing the edge crack by convective cooling. Consequently, very high tensile stresses developed near the cooled surfaces resulting in severe damage. The analysis of the problem is worked out using the superposition technique and the principle of quasi-static thermoelasticity behavior. The Fourier integral transform technique is used to solve the crack problem resulting in a singular integral equation of Cauchy type with the derivative of the crack surface displacement as unknown function which is solved numerically. Some numerical values of the transient stress intensity factors for two material combinations are obtained for both edge crack and crack terminating at the interface and demonstrated in terms of time, crack length, coefficient of heat transfer and thickness ratio.

KEY WORDS

Fracture Mechanics, Stress Intensity Factor, Thermal stresses, Layered Materials, Convective Heat Transfer.

* Associate professor, Dept. of Science in Engineering, Faculty of Engineering, International Islamic University, Malaysia, Kuala Lumpur, Malaysia.

INTRODUCTION

The studying of thermoelastic crack problems for multi-layered structure components with different thermomechanical properties is quite important, since these components are used extensively in many engineering applications. Due to sudden cooling, very high tensile stresses will be generated near the cooled surface leading to severe damage. The degree of the severity can be measured in terms of the stress intensity factor, which is an important parameter to predict mechanical failure for subcritical crack growth, as a function of time and the crack length as well as the materials properties of the composite medium. The crack problems in an elastic plate under thermal loading have been investigated by many researchers [1-7]. The investigation of multi-layered cracked problems under thermal loading has also been considered in the literature [8-15]. The crack problem for a coated layer bonded to substrate under thermal stresses was discussed in [8]. The problem of coated plates on an elastic foundation and shells under thermal shock was investigated in [9]. The problem of two parallel cracks in two bonded dissimilar elastic half-planes was considered in [10].The transient thermal stress problem for a cladded medium containing an underclad crack bonded to a substrate via transitional layer was analyzed in [11]. The problem of collinear embedded cracks in a layered medium consisting of a surface layer and a semi-infinite substrate bonded through an interfacial zone with graded properties was examined [12]. The thermoelastic problem of steady-state heat flow disturbed by a crack perpendicular to the graded interfacial zone bonded by two homogenous half planes was studied in [13]. The crack problem in the nonhomogeneous interfacial zone between two dissimilar elastic half-planes was considered in [14].

In the present paper, the study of the three layered materials with edge cracks and cracks terminating at the interface located symmetrically in the outer similar coated layers bonded to a homogenous layer along an ideal plane interface subjected to thermal stresses is considered. The thermal stresses are caused by convective cooling on the surfaces containing the cracks. The main assumption of this study is: the thermoelastic coupling effects and the possible dependence of the thermoelastic coefficients on the temperature are negligible. Also the problem is treated as quasi-static, i.e. the inertia effects are negligible. The superposition principle is used to formulate the problem that is the solution of the problem is considered as the sum of two solutions. The first solution is obtained for the thermoelastic problem without cracks. The second solution is obtained for the isothermal crack problem (mixed boundary value problem) in which the equal and opposite sign of the thermal stresses given by the first problem are the only external loads acting on the crack surfaces. Since we are concerned with the stress intensity factor, it is sufficient to consider the cracked medium only. The perturbation problem is formulated by expressing the displacement components in terms of Fourier integral transform. Then by defining a new function as the derivative of the crack surface displacement, the problem will be reduced to a singular integral equation of Cauchy type which is solved numerically utilizing the expansion method technique [15, 16]. Numerical results of the stress intensity factors are calculated for edge crack and crack terminated at the interface for two different material combinations namely composite A and composite B and demonstrated as a function of normalized time (Fourier number), normalized crack length, normalized coefficient of heat transfer (Biot number), and the thickness ratio. The composite A represents a stainless steel (outer layers) welded on a ferritic steel (inner layer) with the same mechanical properties but different thermal properties and

the composite B stands for a ceramic (outer layers) coating on ferritic steel (inner layer) in which the mechanical and the thermal properties are different.

FORMULATION OF THE PROBLEM

The three-layered composite medium considered is depicted in Fig.1. The inner layer of thickness $2h_2$ is bonded to two similar coated layers of thickness h_1. Each layer contains a crack normal to the surfaces of length $l = b - a$ located symmetrically. It was assumed that the medium was at uniform temperature T_o. At $t = 0$, the surfaces $x = 0$ and $x = 2h_1 + 2h_2$ of the composite are quenched by a convective cooling with ambient temperature T_a. The case of an edge crack will be considered by letting $a \to 0$. Since the plane $x = h_1 + h_2$ is the plane of symmetry for loading and geometry, the problem may be considered for $0 < x < h_1 + h_2$. Notice that the symmetric plane $x = h_1 + h_2$ will be treated as an insulated plane. The transient thermal stresses for uncracked medium can be obtained by solving first the diffusion equations with proper initial and boundary conditions which are given by

$$\frac{\partial^2 \theta_i(x,t)}{\partial x^2} = \frac{1}{D_i}\frac{\partial \theta_i(x,t)}{\partial t}\ , \ (i = 1, 2), \tag{1}$$

$$\theta_i(x,0) = 0, \quad (i = 1, 2) \quad , \quad k_1^{'}\frac{\partial \theta_1(0,t)}{\partial x} = h\,[\theta_1(0,t) - \theta_o], \tag{2}$$

$$\theta_1(h_1,t) = \theta_2(h_1,t) \qquad , \quad k_1^{'}\frac{\partial \theta_1(h_1,t)}{\partial x} = k_2^{'}\frac{\partial \theta_2(h_1,t)}{\partial x}, \quad \frac{\partial \theta_2(h_1+h_2,t)}{\partial x} = 0, \tag{3}$$

where $\theta_i(x,t) = T_i(x,t) - T_o$, $(i = 1, 2)$, $\theta_o = T_a - T_o$, h is the coefficient of heat transfer, and $k_i^{'}$, D_i $(i = 1, 2)$ are the coefficients of thermal conductivity and the thermal diffusivity, respectively. By using Laplace transform technique in straight forward manner [17] the transient temperature distribution may be given as

$$\frac{\theta_1(x^*,\tau)}{\theta_o} = 1 - 2\sum_{n=1}^{\infty}\frac{1}{\lambda_n}\frac{e^{-\tau\lambda_n^2}\,[\cos\lambda_n(x^*-1)\cos(\delta R\lambda_n) + \eta\sin\lambda_n(x^*-1)\sin(\delta R\lambda_n)]}{[(\lambda_n/Bi)(1+\eta\delta R)\cos\lambda_n\cos(\delta R\lambda_n) - (\lambda_n/Bi)(\eta+\delta R)\sin\lambda_n\sin(\delta R\lambda_n)}$$
$$\frac{1}{+((1/Bi)+1+\eta\delta R)\sin\lambda_n\cos(\delta R\lambda_n) + ((\eta/Bi)+\delta R+\eta)\cos\lambda_n\sin(\delta R\lambda_n)]}, \ 0 \le x^* \le 1, \tag{4}$$

$$\frac{\theta_2(x^*,\tau)}{\theta_o} = 1 - 2\sum_{n=1}^{\infty}\frac{1}{\lambda_n}\frac{e^{-\tau\lambda_n^2}\,[\cos\delta\lambda_n(x^*-1)\cos(\delta R\lambda_n) + \sin\delta\lambda_n(x^*-1)\sin(\delta R\lambda_n)]}{[(\lambda_n/Bi)(1+\eta\delta R)\cos\lambda_n\cos(\delta R\lambda_n) - (\lambda_n/Bi)(\eta+\delta R)\sin\lambda_n\sin(\delta R\lambda_n)}$$
$$\frac{1}{+((1/Bi)+1+\eta\delta R)\sin\lambda_n\cos(\delta R\lambda_n) + ((\eta/Bi)+\delta R+\eta)\cos\lambda_n\sin(\delta R\lambda_n)]}, 1 \le x^* \le 1+R, \tag{5}$$

where $x^* = x/h_1$, $\tau = tD_1/h_1^2$ (Fourier number), $\eta = (k_2^{'}/k_1^{'})\sqrt{D_1/D_2}$, $R = h_2/h_1$ (thickness ratio), $\delta = \sqrt{D_1/D_2}$, $Bi = hh_1/k_1^{'}$ (Biot number), and λ_n are the roots of the transcendental equation

$$Bi[\cos\lambda_n \cos(\delta R\lambda_n) - \eta \sin\lambda_n \sin(\delta R\lambda_n)] = \lambda_n [\sin\lambda_n \cos(\delta R\lambda_n) + \eta \cos\lambda_n \sin(\delta R\lambda_n)] \quad (6)$$

Because of symmetry, the medium would be remaining flat under self-equilibrating transient thermal stresses, i.e. it undergoes uniform strain $\varepsilon_o(t)$ in $y-$ and $z-$directions and the following conditions for the thermal stresses and strains would be satisfied [18]

$$\varepsilon_{ixy}^T = \varepsilon_{ixz}^T = \varepsilon_{iyz}^T = \sigma_{ixy}^T = \sigma_{ixz}^T = \sigma_{iyz}^T = 0\,,\ (i=1,2)\,, \quad (7)$$

$$\varepsilon_{iyy}^T = \varepsilon_{izz}^T\,,\ \sigma_{iyy}^T = \sigma_{izz}^T\,,\ \sigma_{ixx}^T = 0\,,\ (i=1,2)\,, \quad (8)$$

$$\varepsilon_{iyy}^T(x,t) = \varepsilon_{izz}^T(x,t) = \varepsilon_o(t)\,,\ (i=1,2)\,. \quad (9)$$

Also, in the absence of external loads, the thermal stresses would satisfy no resultant force in $y-$ and $z-$ directions, i.e.

$$\int_0^{h_1} \sigma_{1yy}^T(x,t)\,dx + \int_{h_1}^{h_1+h_2} \sigma_{2yy}^T(x,t)\,dx = 0\,, \qquad \int_0^{h_1} \sigma_{1zz}^T(x,t)\,dx + \int_{h_1}^{h_1+h_2} \sigma_{2zz}^T(x,t)\,dx = 0 \quad (10)$$

By using the strain-stress relations and the conditions (7-9) it follows that

$$\sigma_{iyy}^T(x,t) = \sigma_{izz}^T(x,t) = \frac{E_i}{1-\upsilon_i}[\varepsilon_o(t) - \alpha_i'\theta_i(x,t)]\,,\ (i=1,2)\,, \quad (11)$$

where

$$\varepsilon_o = \frac{\left(\frac{E_1}{1-\upsilon_1}\right)\alpha_1' h_1 \overline{\theta_1} + \left(\frac{E_2}{1-\upsilon_2}\right)\alpha_2' h_2 \overline{\theta_2}}{\left(\frac{E_1}{1-\upsilon_1}\right)h_1 + \left(\frac{E_2}{1-\upsilon_2}\right)h_2}\,,\quad \overline{\theta_1} = \frac{1}{h_1}\int_0^{h_1}\theta_1(x,t)\,dx\,,\quad \overline{\theta_2} = \frac{1}{h_2}\int_{h_1}^{h_1+h_2}\theta_2(x,t)\,dx \quad (12)$$

The partial differential equations for solving the plane crack problem are given by

$$(\kappa_i - 1)\nabla^2 u_i + 2\left(\frac{\partial^2 u_i}{\partial x^2} + \frac{\partial^2 v_i}{\partial x \partial y}\right) = 0\,,\quad (i=1,2)\,, \quad (13)$$

$$(\kappa_i - 1)\nabla^2 v_i + 2\left(\frac{\partial^2 u_i}{\partial x \partial y} + \frac{\partial^2 v_i}{\partial y^2}\right) = 0\,,\quad (i=1,2)\,, \quad (14)$$

where $\kappa_i = (3-4\upsilon_i)\,,\ (i=1,2)$, for plane strain, and $u_i, v_i\,,\ (i=1,2)\,,$ are the x and y components of the displacement vectors respectively. Because of symmetry, the problem is considered for $0 < y < \infty$ which is subjected to the following conditions

$$\sigma_{1xx}(0,y) = 0\,,\quad \sigma_{1xy}(0,y) = 0\,, \quad (15)$$

$$\sigma_{1xx}(h_1,y)=\sigma_{2xx}(h_1,y)\,,\qquad \sigma_{1xy}(h_1,y)=\sigma_{2xy}(h_1,y)\,, \tag{16}$$

$$u_1(h_1,y)=u_2(h_1,y)\,,\qquad v_1(h_1,y)=v_2(h_1,y)\,, \tag{17}$$

$$\sigma_{2xy}(h_1+h_2,y)=0\,,\qquad u_2(h_1+h_2,y)=0\ , \tag{18}$$

$$\sigma_{1xy}(x,0)=0\,,\ \ 0<x<h_1\,,\ \text{and}\ \ \sigma_{2xy}(x,0)=0\,,\ v_2(x,0)=0\,,\ \ h_1<x<h_1+h_2\,, \tag{19}$$

$$u_i(x,y)\to 0\,,\ v_i(x,y)\to 0\,,\ \ (i=1,2)\ \text{as}\ \ y\to\infty \tag{20}$$

$$v_1(x,0)=0\ \ ,\ 0<x<a,\ \ b<x<h_1\,,\ \ \ \sigma_{1yy}(x,0)=-\sigma_{1yy}^{T}(x,t)\ \ \ ,a<x<b\,. \tag{21}$$

By expressing the displacement components $u_i, v_i\,,\ (i=1,2)\,,$ in terms of Fourier integral transform as follows

$$u_i(x,y)=\frac{2}{\pi}\int_0^{\infty}A_i(x,\alpha)\cos\alpha\, y\,d\alpha+\frac{1}{2\pi}\int_{-\infty}^{\infty}B_i(y,\beta)e^{ix\beta}d\beta\,,\ \ (i=1,2)\,, \tag{22}$$

$$v_i(x,y)=\frac{2}{\pi}\int_0^{\infty}F_i(x,\alpha)\sin\alpha\, y\,d\alpha+\frac{1}{2\pi}\int_{-\infty}^{\infty}G_i(y,\beta)e^{ix\beta}d\beta\,,\ \ (i=1,2)\,, \tag{23}$$

and defining the new unknown function $\varphi(x)=\partial v_1(x,0)/\partial x$, the mixed boundary value problem described by Eqs. (15) - (23) will be reduced to the following singular integral equation:

$$\int_a^b\frac{\varphi(s)}{(s-x)}\,ds+\int_a^b k_1(x,s)\varphi(s)\,ds=-\frac{\pi(\kappa_1+1)}{4\mu_1}\sigma_{1yy}^{T}(x,t)\,,\qquad a<x<b\,, \tag{24}$$

where the kernel $k_1(x,s)$ is of the form:

$$k_1(x,s)=\int_0^{\infty}G(x,s,\alpha)\,d\alpha\,. \tag{25}$$

where $G(x,s,\alpha)$ is given in Appendix A. By examining the kernel $k_1(x,s)$ as $\alpha\to\infty$, some terms are unbounded as $x\to 0$ and $x\to h_1$ (generalized Cauchy kernels). So $k_1(x,s)$ can be written in the form:

$$k_1(x,s)=k_1^{b}(x,s)+k_{1a}^{s}(x,s)+k_{1b}^{s}(x,s)\,, \tag{26}$$

where $k_1^{b}(x,s)$ is bounded in the closed interval $[a,b]$, and $k_{1a}^{s}(x,s)$ and $k_{1b}^{s}(x,s)$ are the singular terms as $a=0$ and $b=h_1$ respectively and they are found to be [8]:

$$k_{1a}^{s}(x,s)=-\frac{1}{s+x}+\frac{6x}{(s+x)^2}-\frac{4x^2}{(s+x)^3}\,, \tag{27}$$

$$k_{1b}^{s}(x,s)=\frac{c_{11}}{2h_1-x-s}+\frac{c_{12}(h_1-x)}{(2h_1-x-s)^2}+\frac{c_{13}(h_1-x)^2}{(2h_1-x-s)^3} \tag{28}$$

where

$$c_{11}=\frac{3(m-1)}{2(m+\kappa_1)}-\frac{(m\kappa_2-\kappa_1)}{2(m\kappa_2+1)},\quad c_{12}=-6\frac{m-1}{m+\kappa_1},\quad c_{13}=4\frac{m-1}{m+\kappa_1},\quad m=\frac{\mu_1}{\mu_2} \tag{29}$$

The singularities of the function $\varphi(x)$ in Eq. (24) at the irregular points a and b can be obtained using the function theoretic method developed by Muskhelishvili technique [19] by letting

$$\varphi(s)=\frac{g(s)}{(s-a)^{\gamma_1}(b-s)^{\gamma_2}}, \tag{30}$$

where $g(s)$ is bounded in the closed interval $[a,b]$ and nonzero at the end points, and γ_1, γ_2 are the strength of the singularity at the end points which should satisfy $0<\mathrm{Re}(\gamma_1,\gamma_2)<1$. Following [19], it can be shown that, as long as we have internal crack in homogenous material (layer 1) $(a>0, b<h_1)$, the singularities at the crack tips are $\gamma_1=1/2$ and $\gamma_2=1/2$. In the case of edge crack $(a=0, b<h_1)$, $\gamma_2=1/2$ and the characteristic equations for γ_1 at $a=0$ may be expressed as

$$\cos\pi\gamma_1-2(\gamma_1-1)^2+1=0, \tag{31}$$

in which the only acceptable root is $\gamma_1=0$. In the case of an edge crack terminating at the interface, the singularity γ_2 would depend on the materials properties through the characteristic equation:

$$\cos\pi\gamma_2-\frac{1}{2}c_{13}\gamma_2(\gamma_2+1)-c_{12}\gamma_2-c_{11}=0, \tag{32}$$

where c_{11}, c_{12}, c_{13} are given by Eq. (29). The mode I stress intensity factor for the edge crack at the end point b is defined by [20]:

$$K(b)=\lim_{x\to b^+}\sqrt{2(x-b)}\,\sigma_{1yy}(x,0) \tag{33}$$

where $\sigma_{1yy}(x,0)$ is the stress outside the crack and can be obtained from Eq. (24). By using Eq. (24) with Eq. (30) into Eq. (33) and discussing the asymptotic analysis given by Muskhelishvili [19], the stress intensity factor for an edge crack at edge b is given by:

$$K(b)=-\frac{4\mu_1}{\kappa_1+1}\sqrt{2}\,g(b). \tag{34}$$

In the case of crack terminating at the interface ($b=h_1$), the stress intensity factor is define by [20]

$$K(b=h_1)=\lim_{x\to h_1^+}\sqrt{2}\,(x-h_1)^{\gamma_2}\,\sigma_{2yy}(x,0)\,, \tag{35}$$

where γ_2 is the singularity given by Eq. (32), and $\sigma_{2yy}(x,0)$ is the stress in layer 2 ($x>h_1$) and is given by

$$\sigma_{2yy}(x,0)=2\mu_2\lim_{y\to 0}\frac{2}{\pi}\int_0^{\infty}[(-C_5\alpha-C_6\frac{\kappa_2+3}{2}-C_6x\alpha)\,e^{x\alpha}+(C_7\alpha-C_8\frac{\kappa_2+3}{2}+C_8x\alpha)\,e^{-x\alpha}]$$
$$\cos y\alpha\; d\alpha\,, \qquad h_1<x<(h_1+h_2)\,, \tag{36}$$

where C_5, C_6, C_7, and C_8 are found in Appendix A. As $\alpha\to\infty$ and $x\to h_1$ some terms in the kernel of Eq. (36) are unbounded $k_{2b}^{s}(x,s)$ and found to be

$$k_{2b}^{s}(x,s)=\frac{d_{21}}{(x-s)}+\frac{d_{22}(x-h_1)}{(x-s)^2}\,, \tag{37}$$

where

$$d_{21}=\frac{m(\kappa_2+1)}{2(m+\kappa_1)}-\frac{3m(\kappa_2+1)}{2(m\kappa_2+1)},\; d_{22}=\frac{m(\kappa_2+1)}{(m\kappa_2+1)}-\frac{m(\kappa_2+1)}{(m+\kappa_1)},\; m=\frac{\mu_1}{\mu_2}\,. \tag{38}$$

Similarly, by using Eq. (36) with Eq. (30) into Eq. (35) and following Muskhelishvili [19], the stress intensity factor at the crack tip $b=h_1$ is given by

$$K(b=h_1)=\frac{4\mu_2}{1+\kappa_2}\sqrt{2}\,\frac{d_{21}+d_{22}\gamma_2}{(h_1-a)^{\gamma_1}\sin\pi\gamma_2}\,g(h_1)\,. \tag{39}$$

The singular integral Eq.(24) is solved numerically using the expansion method developed in [15, 16]. Firstly, Eq.(24) is normalized by introducing the following quantities:

$$s=\frac{b-a}{2}\rho+\frac{b+a}{2}\,,\quad x=\frac{b-a}{2}r+\frac{b+a}{2}\,. \tag{40}$$

which will be in the form

$$\int_{-1}^{+1}\frac{\psi(\rho)}{(\rho-r)(1+\rho)^{\gamma_1}(1-\rho)^{\gamma_2}}\,d\rho+\int_{-1}^{+1}h(r,\rho)\,\frac{\psi(\rho)}{(1+\rho)^{\gamma_1}(1-\rho)^{\gamma_2}}\,d\rho=-\frac{\pi(\kappa_1+1)}{4\mu_1}\,q(r,t)\,, \tag{41}$$

where

$$\psi(\rho)=\left(\frac{2}{b-a}\right)^{\gamma_1+\gamma_2}g(s)\,,\; h(r,\rho)=\frac{b-a}{2}\,k(x,s)\,,\; \sigma_{1yy}^{T}(x,t)=q(\rho,t)\,. \tag{42}$$

Then it is assumed that the unknown function $\psi(\rho)$ may be approximated by the polynomial of finite degree as

$$\psi(\rho) = \sum_{n=0}^{N} a_n \rho^n , \tag{43}$$

where a_n are $(N+1)$ unknown coefficients to be determined. By substituting Eq. (43) into Eq. (41), we end up with a system of linear equations that are solved at particular collocation points which are selected to be the zeros of Chebychev polynomial of degree $(N+1)$ in the form

$$r_j = \cos\frac{\pi(2j-1)}{2(N+1)}, \quad j = 1,2,...N+1 \tag{44}$$

Following the procedure developed by [21], the unknown coefficients of the polynomial can be determined and consequently the stress intensity factors can be evaluated from Eq. (34) and Eq.(39).

RESULTS

In this analysis, the numerical results are obtained for two composite media. The composite A is chosen to be a stainless steel (outer layers 1) welded on ferritic steel (inner layer 2) and the composite B is fabricated from a ceramic (outer layer 1) bonded to a ferritic steel (inner layer 2). Since the analysis has been obtained in normalized quantities, the ratios of the thermoelastic properties for the two composite mediums are given in Table 1.

Figures 2-5 show sample results for the normalized transient thermal stresses defined by $\sigma_{yy}^T(x^*,\tau)/\sigma_o^T$, where $\sigma_o^T = -E_1\alpha_1'\theta_o/(1-\upsilon_1)$, versus the normalized distance x^*/h_1. The results are demonstrated for the composite media A and B, different normalized time (Fourier number, $\tau = tD_1/h_1^2$), two values of thickness ratio ($h_2/h_1 = 3.0, 9.0$), and two different Biot number ($Bi = \infty, 20$, where $Bi = hh_1/k_1'$) where . It can be seen that, for small values of time, the normalized thermal stresses started to be tensile in the region near the cooled surface $x = 0$, and compressive in the region near the plane $x = h_1 + h_2$. By increasing the time τ, the behavior of the thermal stresses will be maintained for the medium A while the opposite sign for the thermal stresses will be taking place for medium B (compressive near the cooled surface $x = 0$ and tensile near the plane $x = h_1 + h_2$). Note that, at any instant of time, the condition of zero resultant force in $y-$direction is satisfied. It is clear that, for small time, the gradient of the thermal stresses is very high and it becomes less as the time increases. For the steady state condition ($\tau \to \infty$), the thermal stresses for both medium A and B become constant as given by Eq. (11) with discontinuity at the interface due to the dissimilarity of the thermoelastic properties of the composite materials. The effect of the Biot number on the normalized thermal stresses is quite obvious in these figures by reducing the normalized thermal stresses as the Biot number decreases and the highest thermal stresses will arise for the unit step function temperature change

($Bi = \infty$). Also, the figures demonstrate the influence of the thickness ratio h_2 / h_1 on the normalized thermal stresses via increasing the normalized thermal stresses as h_2 / h_1 increases.

Figures 6-7 show the variation of the normalized stress intensity factors for an edge crack defined by $K(b)/\sigma_o^T \sqrt{b}$ calculated from Eq. (34) versus normalized time $\tau = tD_1 / h_1^2$ for the two composite media A and B, different normalized crack length $b/h_1 = 0.01, 0.1, 0.2, 0.5, 0.9$, two values of Biot number $Bi = \infty, 20$, and two values of thickness ratio $h_2 / h_1 = 3.0, 9.0$. Apparently, the normalized stress intensity factor starts to increase as the normalized time τ increases until it reaches a maximum value and then decreases as τ increases for all normalized crack lengths. This performance mainly depends on the distribution of the thermal stresses on the crack surfaces as shown in Figs. 2-5. The highest values of the normalized stress intensity factors will occur for small crack length and decrease as the crack length increases due to the reduction in the thermal stresses as shown in Figs. 2-5. Also as a result of the variation of the normalized thermal stresses, the normalized stress intensity factors are always positive at any time τ for composite medium A while for composite medium B, the normalized stress intensity factor starts to be positive and then negative as τ increases. The effect of the Biot number and the thickness ratio on the normalized stress intensity factor is also shown in the same figures by reducing the normalized stress intensity factor as the Biot number decreases and thickness ratio decreases.

To see quantitatively the effect of the Biot number on the stress intensity factor, Fig. 8 shows the normalized stress intensity factor versus normalized time for different values of Biot number $(Bi = \infty, 20, 10, 5, 1)$, one normalized crack length $b/h_1 = 0.5$, and two values of thickness ratio ($h_2 / h_1 = 3.0, 9.0$). The results are depicted for both composite A and B. As shown in the figure, the normalized stress intensity factor would be reduced by reducing the Biot number and the maximum value is delayed as well.

In the case of the edge crack terminating at the interface $b/h_1 = 1.0$, the variation of the normalized stress intensity factor defined by $K(b)/\sigma_o^T\, b^{\gamma_2}$ as a function of normalized time τ is presented in Fig. 9 for different Biot numbers $(Bi = \infty, 20, 10, 5, 1)$, two different thickness ratio ($h_2 / h_1 = 3.0, 9.0$), and two different composite media A and B. As shown from Eq. (32), the singularity (γ_2) at the crack tip $b = h_1$ depends on the elastic properties of the materials combination. Since the elastic properties of the materials for composite A are the same ($E_1 = E_2$ and $\upsilon_1 = \upsilon_2$), then the singularity at the crack tip $b = h_1$ has a square root singularity ($\gamma_2 = 0.5$) while the elastic properties of the materials for composite B are different and therefore the singularity at the crack tip will be given by $\gamma_2 = 0.552538$. The influence of the Biot number and the thickness ratio on the normalized stress intensity factor is also shown in the same figure.

CONCLUSION

In conclusion, the material properties of the composite medium have a great effect on the thermal stresses and consequently on the corresponding stress intensity factor.

Also the Biot Number has a great influence on the normalized stress intensity factor by reducing it as the Biot number decreases. As expected, The highest values of the stress intensity factor are obtained for the unit step function temperature change $(Bi = \infty)$. The normalized stress intensity factor decreases as the normalized crack length increases. Finally, as the thickness ratio h_2 / h_1 increases the normalized stress intensity factor increases as well.

REFERENCES

[1] Nied, H.F., ''Thermal Shock in an Edge-Cracked Plate'', Journal of Thermal Stresses, No.1, pp 217-227, (1983).

[2] Bahr, H,-A., Balke, H., Kuna, M., Liesk, H., ''Fracture Analysis of a Single Edge Cracked Strip under Thermal Shock, Theoretical and Applied Fracture Mechanics'', No. 8, pp 33-39, (1987).

[3] Lam, K.Y., Tay, T.E., Yuan, W.G., ''Stress Intensity Factors of Cracks in Finite Plates Subjected to Thermal Loading'', Engineering Fracture Mechanics, No.43, pp 641-650, (1992).

[4] Fan, X., Yu, S., ''Thermal Shock in a Surface-Cracked Plate'', Engineering Fracture Mechanics, No. 41, pp 223-228, (1992).

[5] Rizk, A.A., ''A Cracked Plate under Transient Thermal Stresses Due to Surface Heating'', Engineering Fracture Mechanics, No. 45, pp 687-696, (1993).

[6] Rizk, A.A., Radwan, S.F., ''Fracture of a Plate under Transient Thermal Stresses'', Journal of Thermal Stresses, No.16, pp 79-102, (1993).

[7] Rizk A.A., ''Edge-Cracked Plate with One Free and One Constrained Boundary Subjected to Sudden Convective Cooling'', Journal of Thermal Stresses, No.17, pp 455-471, (1994).

[8] Rizk, A.A., Erdogan, F., ''Cracking of Coated Materials under Transient Thermal Stresses'', Journal of Thermal Stresses, No.12, pp 125-168, (1989).

[9] Erdogan, F., Rizk, A.A., ''Fracture of Coated Plates and Shells under Thermal Shock'', International Journal of Fracture, No.53, pp159-185, (1992).

[10] Itou, S., Rengen, Q., ''Thermal Stresses Around Two Parallel Cracks in Two Bonded Dissimilar Elastic Half-Planes'', Archive of Applied Mechanics, No.63, pp377-385, (1993).

[11] Choi, H.J., Jin, T.E., Lee, K.Y., ''Transient Thermal Stresses in a Cladded Semi-Infinite Medium Containing an Underclad Crack'', Journal of Thermal Stresses, No.18, pp 269-290, (1995).

[12] Choi, H.J., Jin, T.E., Lee, K.Y., ''Collinear Cracks in a Layered Half-Plane with a Graded Nonhomogeneous Interfacial Zone-Part II: Thermal Shock Response'', International Journal of Fracture, No. 94, 123-135, (1998).

[13] Choi, H.J., ''Thermoelastic Problem of Steady State Heat Flow Disturbed by a Crack Perpendicular to the Graded Interfacial Zone in Bonded Materials'', Journal of Thermal Stresses 26 (2003) 997-1030.

[14] Itou, S., ''Thermal Stresses Around a Crack in the Nonhomogeneous Interfacial layer Between Two Dissimilar Elastic Half-Planes'', International Journal of Solids and Structures, No.41, pp 923-945, (2004).

[15] Kaya, A.C., Erdogan, F., ''On the Solution of Integral Equations With Strongly Singular Kernels'', Quarterly of Applied Mathematics, No.45,pp 105-122, (1987)

[16] Kaya, A.C., Erdogan, F., "On the Solution of Integral Equations with Generalized Cauchy Kernels", Quarterly of Applied Mathematics, No.45, pp 455-469, (1987).
[17] Carslaw, H.S., Jaeger, J.C., Conduction of Heat in Solids, Oxford University Press, New York, (1950).
[18] Burgreen, D., Elements of Thermal Stress Analysis, C.P. Press, Jamaica, New York, (1971).
[19] Muskhelishvili, N.I., Singular Integral Equations, P. Noordhoff, Groningen, The Netherlands, (1953).
[20] Erdogan, F., "Fracture Problems in Composite Materials", Engineering Fracture Mechanics, No.4, pp 811-840, (1972).
[21] A. Stroud, D. Secrest, Gaussian Quadrature Formulas, Prentice-Hall, New York, 1966.

Table 1 Thermoelastic properties of the composite materials*

Composite mediums	$k_2^{'}/k_1^{'}$	D_2/D_1	$\alpha_2^{'}/\alpha_1^{'}$	E_2/E_1	υ_2/υ_1
A	3	3	o.75	1	1
B	3.385	4.07	2.2939	0.6111	1

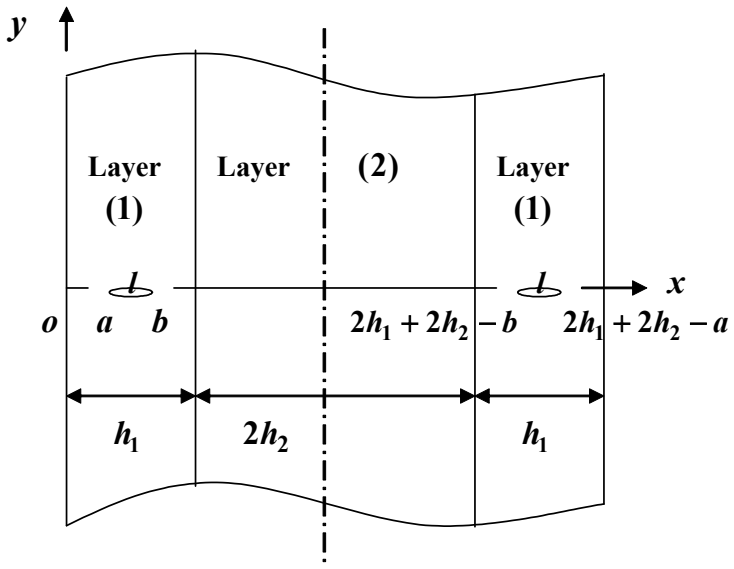

Fig.1 Composite arrangement and crack geometry

* Subscript 1 refers to layer (1) and subscript 2 refers to layer (2)

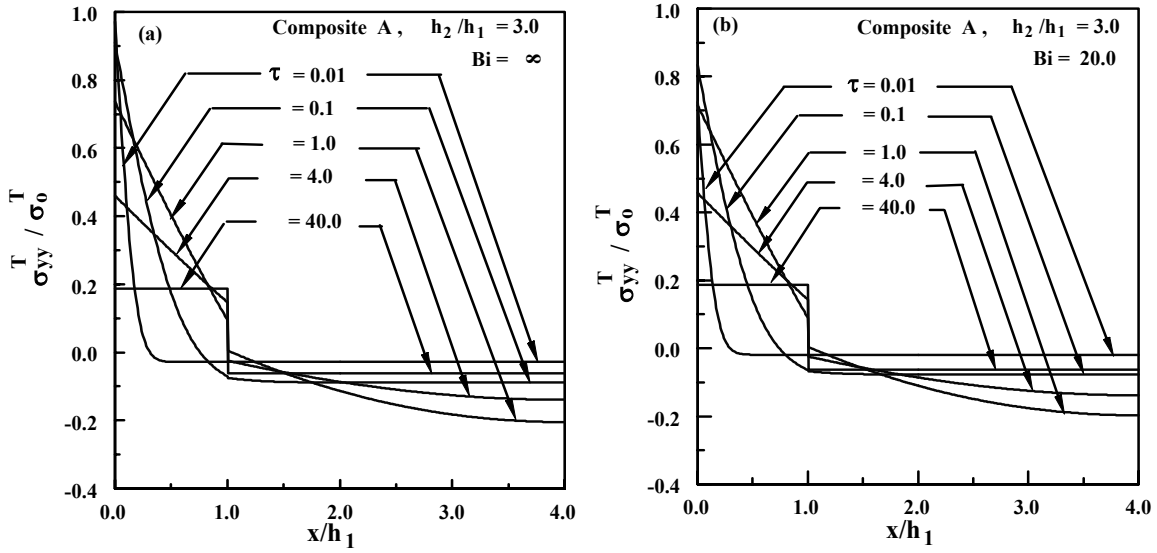

Fig. 2 Transient thermal stresses for $h_2 / h_1 = 3.0$, Composite A (a) $Bi = \infty$, (b) $Bi = 20$

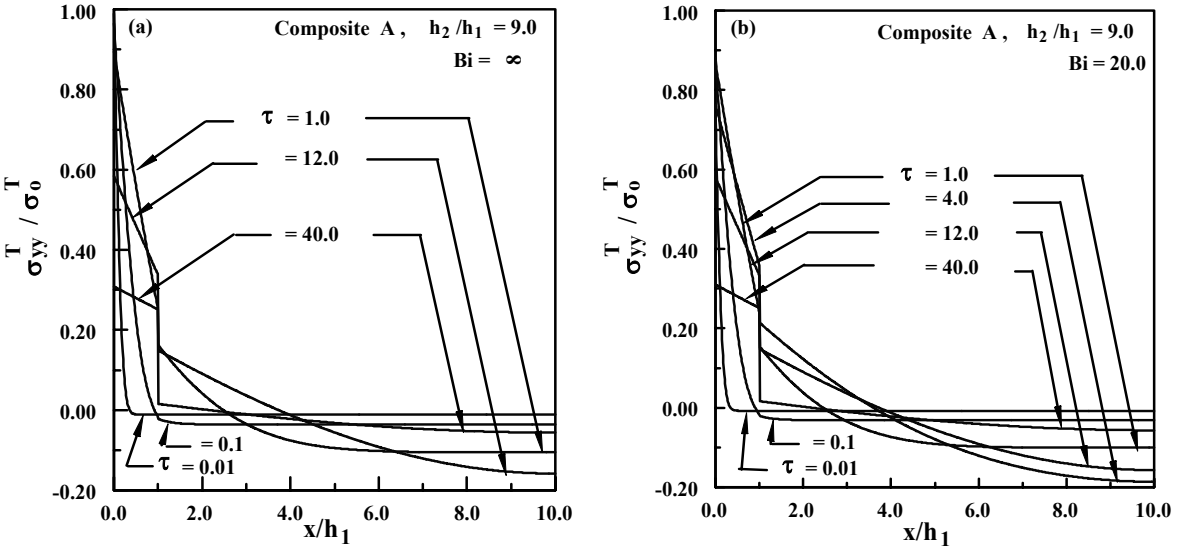

Fig. 3 Transient thermal stresses for $h_2 / h_1 = 9.0$, Composite A (a) $Bi = \infty$, (b) $Bi = 20$

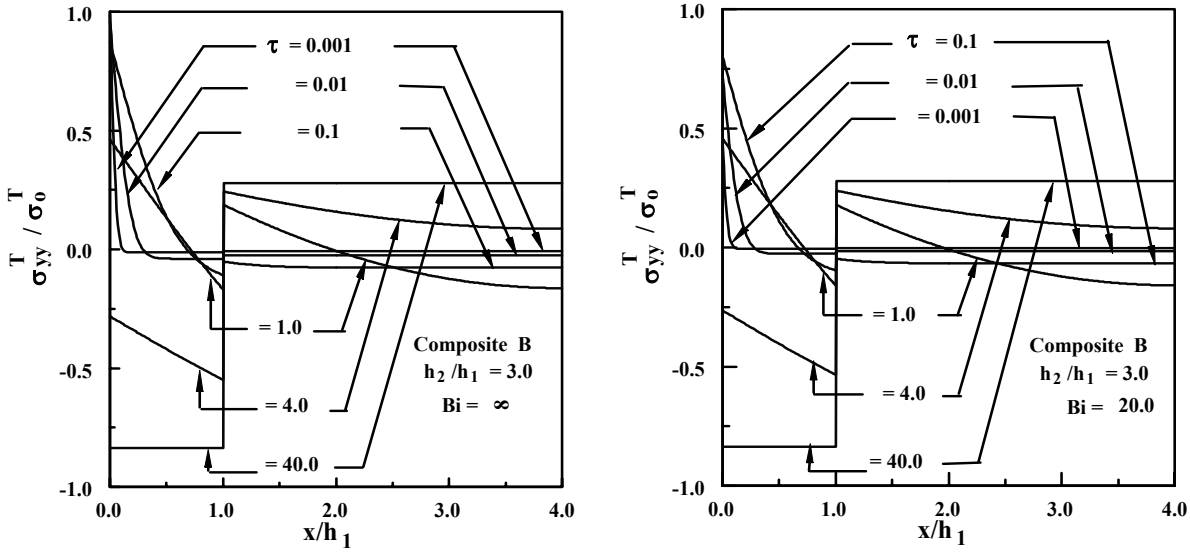

Fig.4 Transient thermal stresses for $h_2 / h_1 = 9.0$, Composite B (a) $Bi = \infty$, (b) $Bi = 20$

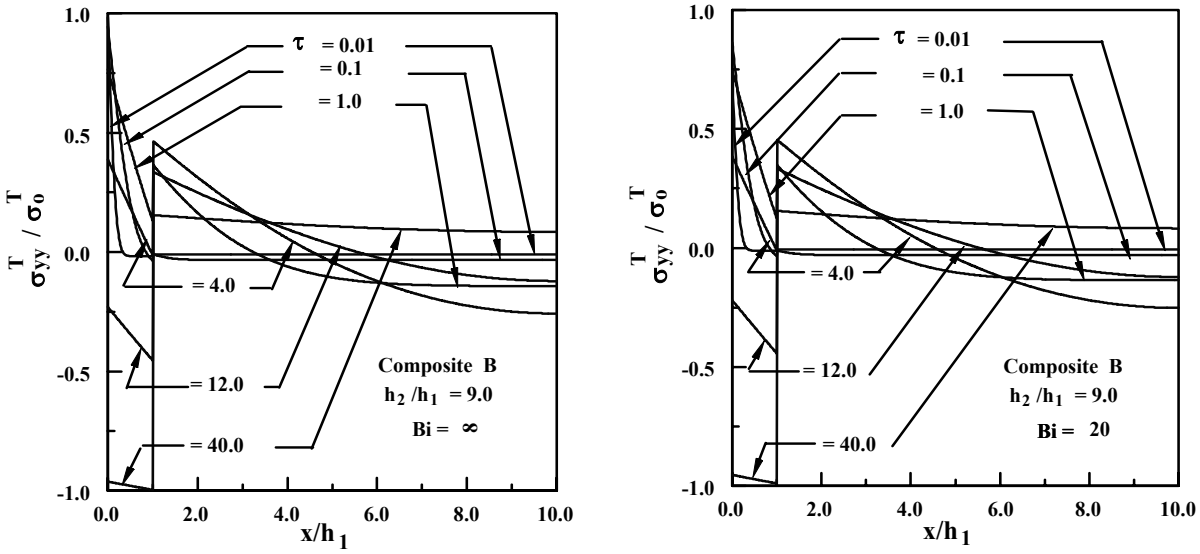

Fig.5 Transient thermal stresses for $h_2/h_1 = 9.0$, Composite B (a) $Bi = \infty$, (b) $Bi = 20$

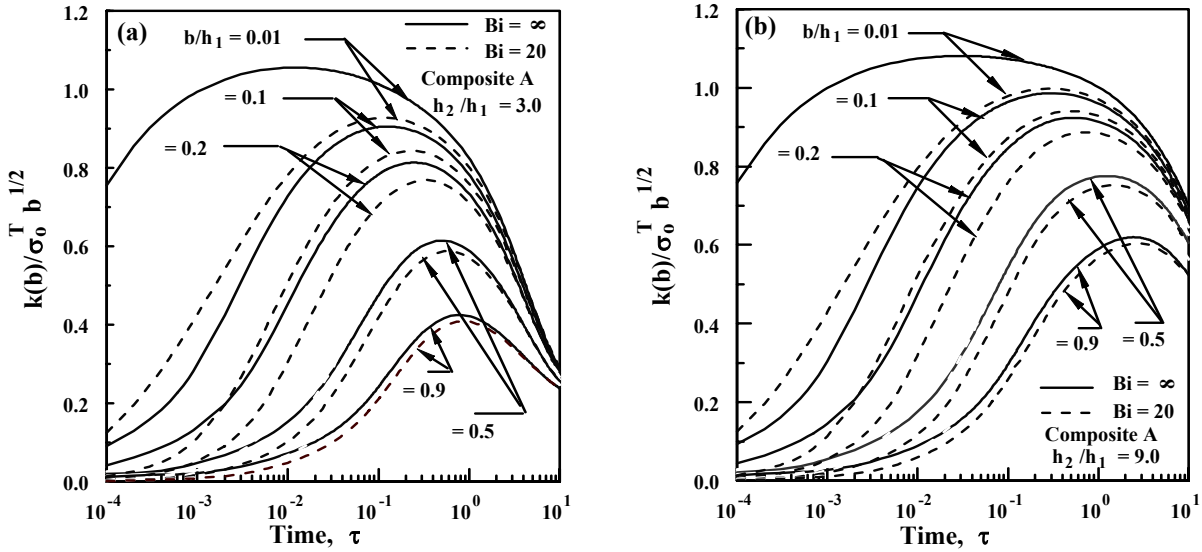

Fig. 6 Stress intensity factors for $Bi = \infty, 20$, Composite A (a) $h_2/h_1 = 3.0$, (b) $h_2/h_1 = 9.0$

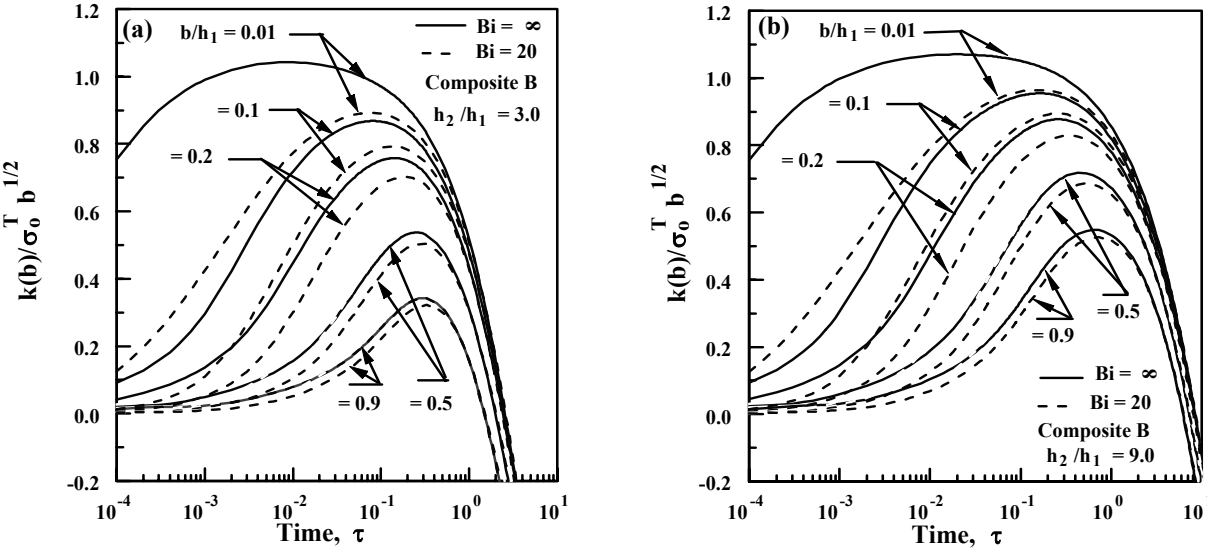

Fig. 7 Stress intensity factors for $Bi = \infty, 20$, Composite B (a) $h_2/h_1 = 3.0$, (b) $h_2/h_1 = 9.0$

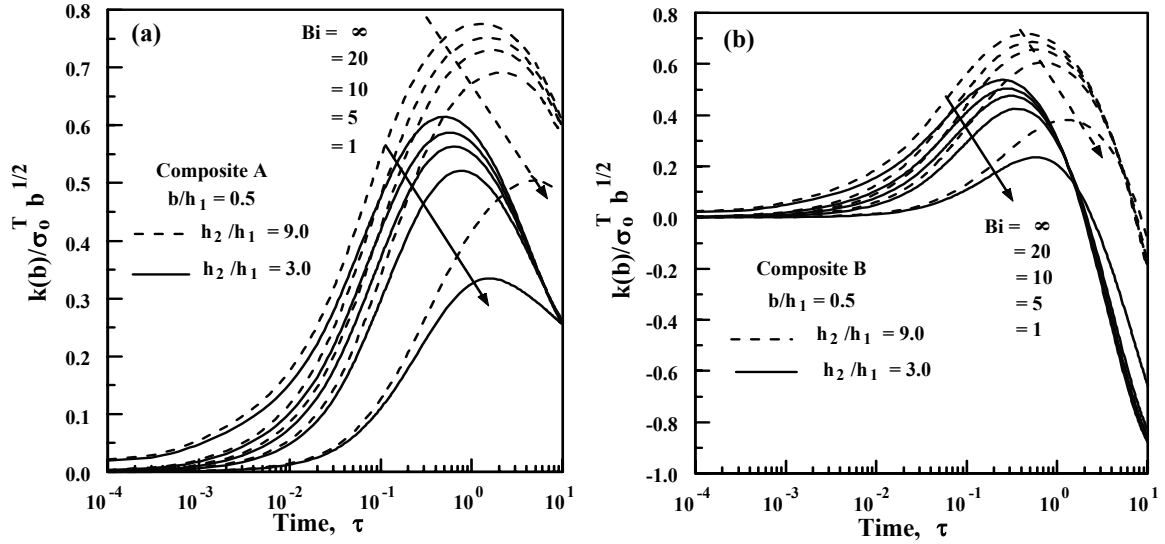

Fig. 8 Stress intensity factors for $h_2 / h_1 = 3.0, 9.0$, $b / h_1 = 0.5$, (a) Comp. A , (b) Comp. B

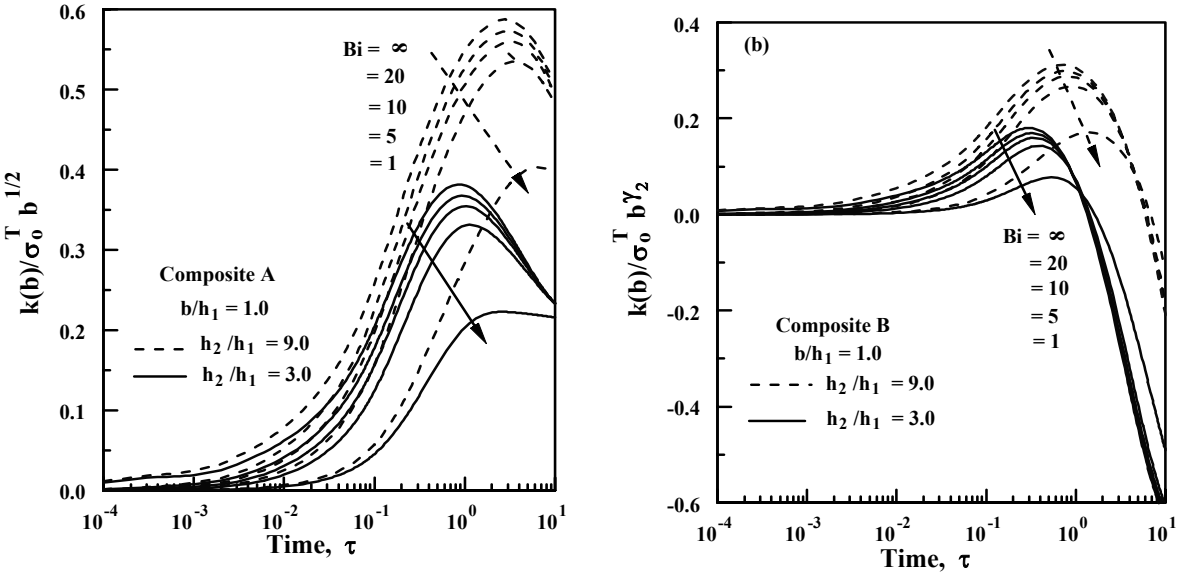

Fig. 9 Stress intensity factors for crack terminating at the interface ($b / h_1 = 1.0$), $h_2 / h_1 = 3.0, 9.0$, (a) Composite A , (b) Composite B

APPENDIX A

$$G(x,s,\alpha) = \frac{1}{D}\left[[-H_1 - (\frac{\kappa_1 + 3}{2} + \alpha x)H_2]e^{x\alpha} + [H_3 - (\frac{\kappa_1 + 3}{2} - \alpha x)H_4]e^{-x\alpha}\right]$$

where

$$H_1 = \frac{1}{2}[-\kappa_1 H_2 + H_4 + D(1 - 2\alpha s)e^{-\alpha s}]$$

$$H_2 = [d_4 d_3 (2\alpha h_2)(1+2\alpha s)]\, e^{(s-4h_1-2h_2)\alpha} + [(-0.5)(d_2 d_3)(1+2\{s-h_1\}\alpha)]\, e^{(s-2h_1-4h_2)\alpha}$$
$$+ [(0.5)(d_2 d_4)(1+2\alpha s)]\; e^{(s-4h_1-4h_2)\alpha}$$
$$+ [-(d_3 d_3)(2\alpha h_2)(1+2\{s-h_1\}\alpha) + (0.5)(d_6 d_5)]\, e^{(s-2h_1-2h_2)\alpha}$$
$$+ [(0.5)(d_6 d_5)(2\alpha s-1) \; + (d_3 d_3)(2\alpha h_2)(2\alpha h_1\{2\alpha s-1\}+1)] e^{-(s+2h_1+2h_2)\alpha}$$
$$+ [(0.5)(d_2 d_3) + (0.5)(d_2 d_3)(2\alpha h_1)(2\alpha s-1)] e^{-(s+2h_1+4h_2)\alpha}$$
$$+ [(0.5)(d_1 d_3)] e^{-(s+4h_1)\alpha} + [-(d_4 d_3)(2\alpha h_2)] e^{-(s+4h_1-2h_2)\alpha}$$
$$+ [(-0.5)(d_2 d_3) + (-0.5)(d_2 d_3)(2\alpha h_1)(2\alpha s-1)] e^{-(s+2h_1)\alpha}$$
$$+ [(-0.5) d_2 d_4]\, e^{-(s+4h_1+4h_2)\alpha} + [(-0.5)(d_1 d_3)(1+2\alpha s)] e^{(s-4h_1)\alpha}$$
$$+ [(0.5)(d_2 d_3)(1+2\{s-h_1\}\alpha)] e^{(s-2h_1)\alpha}$$

$$H_3 = \frac{1}{2}[-H_2 + \kappa_1 H_4 + D e^{-\alpha s}]$$

$$H_4 = [(-0.5)(d_6 d_5)(2\alpha h_1) - (d_4 d_4)(2\alpha h_2) + (0.5)(d_6 d_5)(1+2\{s-h_1\}\alpha)$$
$$+ (d_3 d_3)(2\alpha h_1)(2\alpha h_2)(1+2\{s-h_1\}\alpha)] e^{(s-2h_1-2h_2)\alpha}$$
$$+ [(0.5)(d_4 d_1) - (0.5)(d_2 d_3)(2\alpha h_1)(1+2\{s-h_1\}\alpha)]\, e^{(s-2h_1)\alpha}$$
$$+ [(-0.5)(d_1 d_3)]\, e^{(s-4h_1)\alpha}$$
$$+ [(-0.5)(d_4 d_1) - (0.5)(d_4 d_1) + (0.5)(d_2 d_3)(2\alpha h_1)(1+2\{s-h_1\}\alpha)]\, e^{(s-2h_1-4h_2)\alpha}$$
$$+ [(d_4 d_3)(2\alpha h_2)]\, e^{(s-4h_1-2h_2)\alpha} + [(0.5)(d_4 d_2)]\, e^{(s-4h_1-4h_2)\alpha}$$
$$+ [(-0.5)(d_1 d_3)(2s\alpha-1)]\, e^{-(s+4h_2)\alpha} + [-(d_4 d_3)(2\alpha h_2)(2s\alpha-1)]\, e^{-(s+2h_2)\alpha}$$
$$+ [-(d_3 d_3)(2\alpha h_2)(1-2\{s-h_1\}\alpha) - (0.5)(d_6 d_5)]\, e^{-(s+2h_1+2h_2)\alpha}$$
$$+ [(-0.5)(d_2 d_4)(2\alpha s-1)]\, e^{-(s)\alpha} + [(0.5)(d_2 d_3)(1-2\{s-h_1\}\alpha)]\, e^{-(s+2h_1)\alpha}$$
$$+ [(-0.5)(d_2 d_3)(1-2\{s-h_1\}\alpha)]\, e^{-(s+2h_1+4h_2)\alpha}$$

$$H_5 = \frac{1}{2}[\frac{d_6}{d_3} e^{-(2h_1)\alpha} H_4 - (\kappa_2 + 2\alpha h_1) H_6 - \frac{d_2}{d_3} e^{-(2h_1)\alpha} H_8 + \frac{d_6}{d_3} D e^{(s-2h_1)\alpha}]$$

$$H_6 = \frac{1}{d_5}[(d_4 - d_3\, e^{-2h_1\alpha}) H_2 + d_3 (2\alpha h_1) e^{-2h_1\alpha} H_4 + d_3 D e^{-(s+2h_1)\alpha} - d_3 D(1+2\{s-h_1\}\alpha) e^{(s-2h_1)\alpha}]$$

$$H_7 = \frac{1}{2}[-\frac{d_6}{d_3} e^{(2h_1)\alpha} H_2 + \frac{d_2}{d_3} e^{(2h_1)\alpha} H_6 + (\kappa_2 - 2h_1\alpha) H_8]$$

$$H_8 = e^{2(h_1+h_2)\alpha} H_6$$

$$D = [(d_6 d_5)(2\alpha h_1) + (d_3 d_3)(2\alpha h_2) + (d_4 d_4)(2\alpha h_2) + (d_3 d_3)(2\alpha h_1)^2 (2\alpha h_2)] e^{-2(h_1+h_2)\alpha}$$
$$+ [(0.5)(d_1 d_4) - (0.5)(d_2 d_3)(1+(2\alpha h_1)^2]\, e^{-(2h_1)\alpha} + [(0.5)(d_1 d_3)]\, e^{-(4h_1)\alpha}$$
$$+ [(-0.5)(d_1 d_3)]\, e^{-(4h_2)\alpha} + [(-d_4 d_3)(2\alpha h_2)]\, e^{-(2h_2)\alpha}$$
$$+ [(0.5)(d_2 d_3)(1+(2\alpha h_1)^2 + (0.5)(d_1 d_4)]\, e^{-(2h_1+4h_2)\alpha}$$
$$+ [(-d_4 d_3)(2\alpha h_2)]\, e^{-(4h_1+2h_2)\alpha} + [(-0.5)(d_2 d_4)] + [(-0.5)(d_2 d_4)]\, e^{-(4h_1+4h_2)\alpha}$$

$$d_1 = m\kappa_2 - \kappa_1,\; d_2 = m\kappa_2 + 1,\; d_3 = m-1,\; d_4 = \kappa_1 + m,\; d_5 = \kappa_2 + 1,\; d_6 = m(\kappa_1 + 1),\; m = \mu_1/\mu_2$$

$$C_5 = \frac{1}{\alpha}\,\frac{1}{\kappa_1+1}\int_a^b \frac{H_5}{D}\varphi(s)\,ds\,,\; C_6 = \frac{1}{\kappa_1+1}\int_a^b \frac{H_6}{D}\varphi(s)\,ds\,,$$

$$C_7 = \frac{1}{\alpha}\;\frac{1}{\kappa_1+1}\int_a^b \frac{H_7}{D}\varphi(s)\,ds\,,\; C_8 = \frac{1}{\kappa_1+1}\int_a^b \frac{H_8}{D}\varphi(s)\,ds$$